FP-LAPW calculations of ground state properties for AlN, GaN and InN compounds

B. Daoudi[1,2,*], M. Sehil[1], A. Boukraa[2], H. Abid[1]

[1] *Applied Materials Laboratory, University of Sidi-Bel-Abbès, 22000 Algeria.*
[2] *Laboratoire de Développement des Energies Renouvelables dans les Zones Arides et Sahariennes, Département de Physique, Université de Ouargla, 30000 Algeria.*

Abstract

We present first-principals all-electrons total-energy calculations concerning structural and electronic properties for the group III-V zinc-blend-like compounds AlN, GaN and InN using the full-potential linearized augmented plane wave (FP-LAPW) approach within the density functional theory (D.F.T) in the local density approximation (L.D.A) and the generalized gradient approximation (G.G.A) for the exchange correlations functional. Moreover, we have calculated bulk properties, including ground-state energies, lattice parameters, bulk modulus, its derivatives, cohesive energy and band structures. We find that the GGA yields improved physical properties for bulk AlN compared to the LDA. For GaN and InN, essentially no improvement is found: the LDA exhibits over binding, whereas the GGA shows a tendency for under binding. The degree of under binding and the overestimation of lattice parameters as obtained within the GGA increase on going from InN to GaN. Band structures are found to be very similar within the LDA and the GGA, for AlN, GaN and InN, therefore, the GGA does not offer any significant advantages.

Keywords: FP-LAPW, LDA, GGA, Semiconductors, Nitride compound.

1. Introduction

The nitrides materials AlN, GaN, InN and their alloys have attracted much attention in recent years due to their great potential for technological applications [1-5]. In the wurtzite (ground-state) structure, AlN, GaN and InN have direct energy band gaps of 6.2, 3.4 and 1.9 eV, respectively [3], ranging from the ultraviolet (UV) to the visible regions of the spectrum, which implies that the $Al_xGa_yIn_{1-x-y}N$ alloy system can be used to fabricate optical devices operating at wavelengths ranging from the red up to the UV. In addition, AlN and GaN have a high melting point, a high thermal conductivity, and a large bulk modulus [6]. These properties, as well as the wide band gaps, are closely related to their strong (ionic and covalent) bonding. These materials can therefore be used for short wavelength light-emitting diodes (LED's) laser diodes, and optical detectors, as well as for high-temperature, high power, and high-frequency devices.

*) Corresponding author: Permanent address: Département de Physique, Université de Ouargla, BP.511, 30000 Alegria. Tel: 213 51 18 60 50 E-mail: Bahmeddaoudi@gmail.com, Abid_hamza@yahoo.fr

As a consequence of the very rapid improvement in both experimental and computational techniques, research on the physical properties of materials and devices has seen much activity in recent years. The higher accuracy that can now be achieved has led to several important discoveries, which in some cases have resulted in a complete reassessment of what seemed established before. In the case of the technologically important III-V compounds, theoretical studies can be most valuable. Many first-principles calculations have been performed using the density-functional theory employing the local density approximation (LDA), either in the all-electron formalism or using the pseudo potential plane-wave approach. Moreover, several calculations have been carried out using *ab-initio* Hartree-Fock methods (HF), which are well known by there computationally time-consuming compared to the LDA, and to significantly overestimate the band gap. It is also well known that the LDA underestimates the band gaps in semiconductors [7, 8], in addition to over binding.

The calculations based on density functional theory employing the generalized gradient approximation (G.G.A) have generally been found to improve the description of total energies, ionization energies, electron affinities of atoms, atomization energies of molecules [9-11] and properties of solids [12-15]. Improvements have also been reported for adsorption energies of ad particles on surfaces [16, 17] and for reaction energy [18, 19].
For transition metal oxides, Dufek et al. [20, 21] reported a significant improvement in the band structure when using the GGA. However, Leung et al. [22] reported no significant change in the band structure between LDA and GGA results for the same materials. Thus the effect of the GGA on the band structure is still unclear.

In view of these disparities, it is important to investigate the effect that the GGA may have on the electronic structure, especially, whether it would lead to perfection in the band gap. This work leads to more understanding of the group-III nitrides bulk materials.
To our knowledge, few published calculations have gone beyond the LDA: In the Wurtzite and Zinc-Blend structures, for AlN [23] and GaN [23-25], the authors are used a *GW* approach and simple quasiparticle schemes for Wurtzite and Zinc-Blend GaN [26]. We mention two other approaches that aim to obtain an improved electronic structure of wide-band-gap semiconductors: the first approach is the self-interaction and relaxation pseudo potentials [27] and the second one is the screened exchange method [28].

We report here lattice constants, bulk modulus and their derivatives, cohesive energies and band structures for AlN, GaN and InN, in both zinc blend and wurtzite structures.

2. Method of calculations

In our calculations, we use the Wien2k [29] all-electron full potential linearized augmented plane wave method (FP-LAPW) code within the local density approximation (L.D.A) and the generalized gradient approximation (GGA 96) proposed by Perdew-Brouke-Ernzerhof [30].
As exchange-correlation potential, we use the Ceperly-Alder[31], parameterized by [32] in order to see the dependence of the structural properties on the exchange correlation potential, since it is known that the gap is highly sensitive to the form of exchange correlation potentials. The scalar relativistic treatment was used for the valence states, whereas the core ones was treated fully relativistically [33] and were self consistently updated at each iteration.
The 3d electrons of Ga and In atoms were treated as part of the valence band, since they are relatively high in energy even though they need quite a large value for the product $R_{MT}K_{max}$ (where R_{MT} is the average radius of the muffin-tin spheres and K_{max} is the maximum value of the wave vector K=k+G), in order to have a suitable number of plane waves to correctly describe these states. We used different sphere radius values for Al, Ga, In and N,

the use of the full-potential ensuring that the calculations are completely independent of the choice of sphere radii.
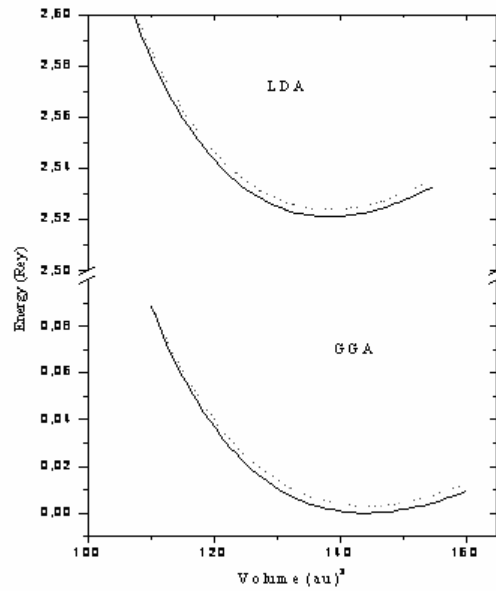

Fig. 1: Total energy versus volume for AlN in the wurtzite (solid curve) and zinc-blende (doted curve) structures.
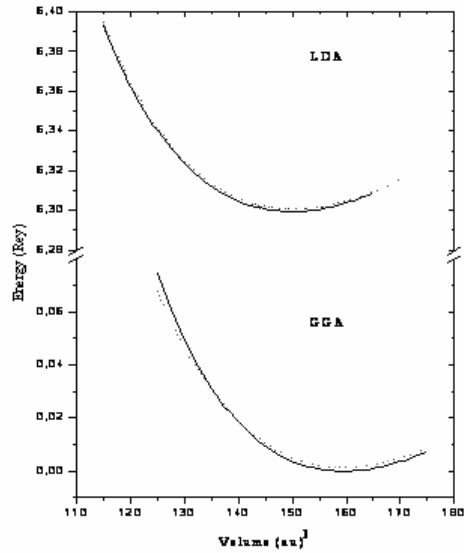

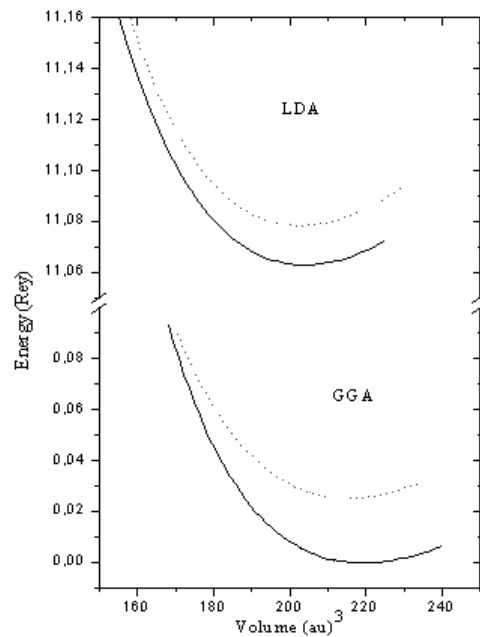Fig. 2: Total energy versus volume for GaN in the wurtzite (solid curve) and zinc-blende (doted curve) structures.

Fig. 3: Total energy versus volume for InN in the wurtzite (solid curve) and zinc-blende (doted curve) structures.

Inside muffin-tin, the sphere radii are R_{MT} =1.65, 1.75, 1.95 and 2.2 *au* for N, Al, Ga, and In, respectively. Atomic orbital up to an angular momentum l =*10* were used to expand the wave functions inside muffin-tin spheres. A satisfactory degree of convergence was achieved by considering a number of (FP-LAPW) basis functions up to $R_{MT}K_{max}$ =9.0. Thus, in order to keep the same degree of convergence for all the lattice constants studied, we kept the values of the sphere radii and of K_{max} constant over all the range of lattice spacing considered. We also mention that the integration in reciprocal lattice space as performed using the special point's method. We use a 10 x 10 x10 mesh (73 **k**-points) for the Zinc-Blend form and a 12 x 12 x 6 mesh (114 **k**-points) for the Wurtzite phase.

3. Results and discussion

We have calculated the total energy curves for the two considered structures (wz and zb) of AlN, GaN, and InN with the GGA and LDA approximations. The ground-state structural parameters have been obtained by minimizing the total energy with respect to the volume. By fitting this total energy versus volume data on the non-linear Murnaghan equation of state [34] as shown in figures.1 to 3, we obtained the lattice parameters, the value of the bulk modulus and its pressure derivative. The results are shown with other values in Tables 1 to 6. The important features to note from these figures are that the wz phase is the ground state structure, and the difference between the ground state energy of the pair (anion, cation) of wz and zb phase is very small (see Tables 1 to 6) due the fact that these two phases have local tetrahedral bonding and they only differ in the second-nearest neighbours. Comparison between the LDA and GGA calculations of the relative stability (energy difference between the wz and zb structures) shows a small but not negligible difference, decreasing on going from AlN to InN to GaN, the same trend as that found in all other studies. The only difference in the magnitude of these values, which is due to the fact that the energy is sensitive to the technical details and approximations used in calculation methods.

3.1. Aluminium nitride

To verify calculations convergence, we calculate the bulk properties of AlN in the zinc-blende structure as a function of $R_{MT}K_{max}$ and special **k**-points. A value below 8.0 for the product of $R_{MT}K_{max}$ and 22 for the **k**-points made the physical quantities poorly converging.

In Tables 1 and 2, we present our calculated bulk properties for AlN in the zinc blende and the wurtzite structures and compare them with some *ab-initio* calculations and experiments. These results were obtained using $R_{MT}K_{max}$ =9.0, with 73 and 114 **k**-points for the zinc blende and wurtzite structures, respectively. Calculations for the zinc-blende structure with 43 **k**-points showed almost identical results, as was the case for GaN and InN.

Table 1 (zinc-blend structure) shows that the lattice constants and the bulk moduli agree well for all calculation methods. We note that for zinc blende AlN the band gap is indirect, while it is direct in wurtzite AlN. From Table 2 (wurtzite structure) it appears that the lattice constants obtained by HF methods are slightly larger than those of the LDA, which is a well-known effect. However, there is no significant difference in the results of physical properties between the all-electron and the pseudo potential methods.

Method	LDA Calculation	a(Å)	B(Mbar)	B'	E_c (eV)	E_g^Γ (eV)
FP-LAPW	Present	4.3464	2.1219	3.77	13.1543	4.356
AE	Ref. [36]	4.32	2.03	3.2		
	Ref. [28]	4.345	2.07			
	Ref. [37]	4.349	2.1178	3.90		
PP-GB	Ref. [27]	4.29				
PP-PW	Ref. [35]	4.310	2.06	3.86	13.242	4.75
	Ref. [38]	4.339	2.04	4.06	17.990	4.50
	Ref. [39]	4.34	2.14	3.3		
	Ref. [40]	4.302	2.10	3.7		
HF	Ref. [44]	4.3742	2.18		10.88	
GW	Ref. [49]					6.0
PP-EXX	Ref. [50]					5.74
	GGA Calculation					
FP-LAPW	Present	4.4066	1.9245	3.80	11.4714	3.961
AE	Ref. [28]	4.40				
PP-PW	Ref. [35]	4.394	1.91	3.81	11.361	4.13
Expt.	Ref. [6]	4.37				

Table 1: Structural properties and band gap at the Γ point of bulk zinc-(blend AlN, calculated at the theoretical lattice constants. Theoretical and experimental values are included for comparison.

Our GGA lattice constants are 1.26% and 1.39% larger than the LDA values, for the wz and the zb structures, respectively. For the wz structure the LDA result is 0.93% smaller than the experimental value, and the GGA result is 0.32% larger, whereas for the zb structure it is 0.54% smaller for the LDA and 0.83% larger for the GGA. The GGA values of the bulk modulus are also smaller than those of the LDA by 9.30% (zb-AlN) and 11.22% (wz-AlN).

The cohesive energies as obtained by the GGA are 1.681 eV (12.79%) and 1.683 eV (12.74%) smaller than the LDA results for the zb and wz structures, respectively. Largely correcting the overbinding of the LDA. The GGA values are therefore in good agreement with experiment.

In Figs. 4 and 5 the band structures of AlN in the zb and the wz structures are calculated at the equilibrium lattice constants for the LDA and the GGA. We see that the band structures are very similar, excepting that the band gaps at Γ for the GGA results are about 0.362 eV (8.15%) and 0.395 (9.07%) smaller than the LDA results for wz and zb structures, respectively. The conduction bands in the GGA calculations are shifted a little down with respect to those of the LDA, but this shift is not constant and depends on the **k**-points. Whereas the valence bands are shifted slightly up, leading to a reduction of the bandwidths. The differences between the LDA and the GGA observed in Figures 4 and 5 are essentially due to differences in the lattice constants (deformation potential effects). Our zb band structures are well compared to those of refs [6] and [35].

Method	LDA Calculation	a(Å)	c(Å)	c/a	u	B(Mbar)	B'	E_c (eV)	E_g^Γ (eV)
FP-LAPW	Present	3.0821	4.9837	1.617	0.379	2.1250	3.93	13.1981	4.44
AE	Ref. [42]	3.072	4.904	1.596	0.382	2.05			
	Ref. [28]	3.091	4.952	1.602	0.381	2.12			
PP-GB	Ref. [27]	3.05	4.89	1.603	0.382				4.2
PP-PW	Ref. [35]	3.057	4.943	1.617	0.380	2.09	5.58	13.286	4.74
	Ref. [39]	3.082	4.945	1.604	0.382	2.15	3.63		
	Ref. [40]	3.061		1.600	0.382	2.09	3.7		
HF	Ref. [43][a]	3.117	4.982	1.598	0.383	2.39	3.77	10.11	
	Ref. [43][b]	3.101	4.975	1.604	0.382	2.39	4.19	11.09	
GW	Ref. [49]								5.8
	GGA Calculation								
FP-LAPW	Present	3.1210	5.0622	1.622	0.378	1.8866	4.65	11.5172	4.078
AE	Ref [28]	3.135	5.022	1.602	0.381				
PP-PW	Ref. [35]	3.113	5.041	1.619	0.380	1.92	3.96	11.403	4.245
Expt.	Refs. [6][36][44]	3.111	4.978	1.601	0.385	1.85-2.12	5.7-6.3	11.669	6.28

Table 2: Structural properties and band gap at the Γ point of bulk wurtzite AlN, calculated at the theoretical lattice
constants. Theoretical and experimental values are included for comparison. [a] All-elctron results, [b] Pseudopotential results

Method	LDA Calculation	a(Å)	B(Mbar)	B'	E_c (eV)	E_g^Γ (eV)
FP-LAPW	Present	4.4637	2.0530	4.29	10.6235	1.922
AE	Ref. [36]	4.46	2.01	3.9		
	Ref. [41]	4.466	1.98		10.88	2.0
	Ref. [37]	4.461	2.02	4.32		
PP-GB	Ref. [27]	4.45				1.60
PP-PW	Ref. [35]	4.518	1.91	4.14	10.179	1.60
	Ref. [45]	4.460	1.87			1.89
	Ref. [25]	4.524	2.06	3.7	10.53	
	Ref. [40]	4.497	1.96	4.2		
HF	Ref. [44]	4.5215	2.54		8.358	
	Ref. [46]	4.510	2.30	3.6		

		a(Å)	B	B'	E_c	E_g
GW	Ref. [49]					3.1
PP-EXX	Ref. [50]					2.88
	GGA Calculation					
FP-LAPW	Present	4.5564	1.7395	3.75	8.7277	1.517
AE	Ref. [28]	4.570				
PP-PW	Ref. [35]	4.590	1.56	4.25	8.253	1.28
Expt.	Refs. [6][36][46]	4.50, 4.531	1.90			3.45, 3.21

Table 3: Structural properties and band gap at the Γ point of bulk zinc blende GaN, calculated at the theoretical lattice constants. Theoretical and experimental values are included for comparison.

Method	LDA Calculation	a(Å)	c(Å)	c/a	U	B(Mbar)	B'	E_c (eV)	E_g^{Γ} (eV)
FP-LAPW	Present	3.1555	5.1528	1.633	0.377	2.0542	4.37	10.6400	2.091
AE	Ref. [36]	3.17	5.13	1.62	0.379	2.07	4.5		
	Ref. [28]	3.160	5.138	1.626	0.377	1.99			
PP-GB	Ref. [27]	3.15	5.13	1.628	0.372				1.70
PP-PW	Ref. [35]	3.193	5.218	1.634	0.376			10.187	1.76
	Ref. [45]	3.162	5.142	1.626	0.377	2.02			2.04
	Ref. [38]	3.196	5.222	1.634	0.375	2.13	4.50	10.547	2.13
	Ref. [40]	3.180		1.632	0.376	1.96	4.3		
HF	Ref. [46]	3.199	5.176	1.618	0.380	2.51	2.7		
	Ref. [44]	3.2011	5.1970	1.6235	0.3775				
GW	Ref. [49]								3.5
	GGA Calculation								
FP-LAPW	Present	3.2241	5.2487	1.628	0.376	1.7238	5.23	8.7462	1.680
PP-PW	Ref. [35]	3.245	5.296	1.632	0.3762	1.72	5.11	8.265	1.46
Expt.	Refs. [6][36][47][44]	3.180-3.192	5.166	1.624	0.375	1.88-2.45	3.2- 4.3	9.058	3.65, 3.44, 3.41

Table 4: Structural properties and band gap at the Γ point of bulk wurtzite GaN, calculated at the theoretical lattice
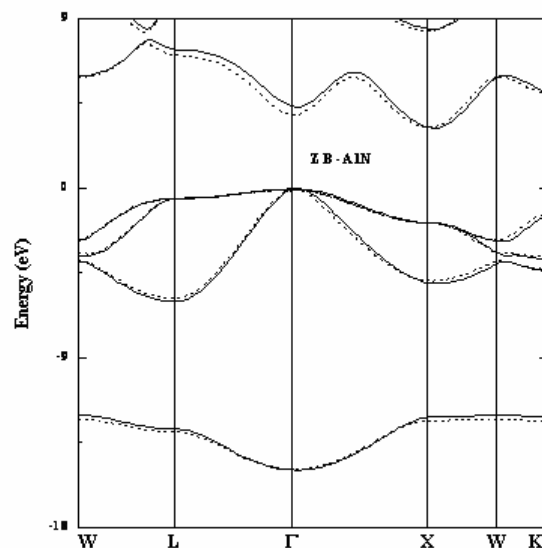constants. Theoretical and experimental values are included for comparison.

Fig. 4: Band structure at the theoretical lattice constants for zinc-blende AlN as obtained using the LDA (solid curve)
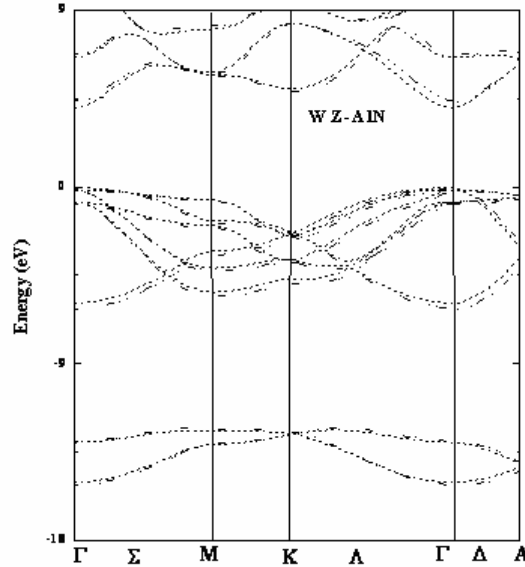and the GGA (dashed curve).

Fig. 5: Band structure at the theoretical lattice constants for wurtzite AlN as obtained using the LDA (solid curve) and the GGA (dashed curve).

3.2. Gallium nitride

As in AlN, and to verify convergence of the calculations, we calculate the bulk properties of GaN in the zb structure as a function of $R_{MT}K_{max}$ and special **k**-points. A value below 8.5 for the product $R_{MT}K_{max}$ and 43 for the special **k**-points in the irreducible part of the Brillouin zone, the physical quantities converge badly.

In Tables 2 and 3 the value of the various bulk properties, listed for the wz and zb structures, are obtained using an $R_{MT}K_{max}$ =9.0 with 114 and 73 special **k**-points, respectively. The lattice constant obtained by the GGA calculations is 2.17% and 2.08% larger than the LDA results, for the wz and the zb structures respectively. Similarly, the bulk modulus is smaller by 16.08% for wz-GaN and 15.27% for zb-GaN. Compared to experiment and for the wurtzite structure the LDA lattice constants value is 1.14% smaller and the GGA one is 1.01% larger, whereas for the zb structure it is 0.81% smaller for the LDA and 1.25% larger for the GGA. The cohesive energies are significantly smaller when we use the GGA rather than the LDA, by 1.894 eV (17.80%) and 1.896 eV (17.85%), for the wz and the zb structures, respectively.

When we compare the calculated cohesive energies to experiment, we find that the GGA values are slightly better than the LDA ones, which indicates an under binding as opposed to

the over binding of the LDA. Consequently, the GGA does not bring about an important improvement over the LDA for GaN.

Method	LDA Calculation	A(Å)	B(Mbar)	B'	E_c (eV)	E_g^Γ(eV)
FP-LAPW	Present	4.9334	1.5367	4.52	8.6048	
AE	Ref. [45]	4.953	1.44			-0.20
	Ref. [36]	4.92	1.39	4.4		
	Ref. [37]	4.947	1.44	4.561		
PP-GB	Ref. [27]	4.97				
PP-PW	Ref. [35]	5.004	1.40	4.38	8.676	-0.40
	Ref. [45]	4.932	1.40			-0.35
	Ref. [38]	4.974	1.49	4.41	8.779	
	Ref. [40]	4.968	1.47	4.4		
HF	Ref. [44]	4.9870	1.59		6.990	
PP-EXX	Ref. [50]					0.81
	GGA Calculation					
FP-LAPW	Present	5.0352	1.2760	4.64	6.7574	
AE	Ref. [28]	5.06				
PP-PW	Ref. [35]	5.109	1.1696	4.4305	6.855	-0.55
Expt.	Ref. [6]	4.98	1.37			

Table 5: Structural properties and band gap at the Γ point of bulk zinc-blend InN, calculated at the theoretical lattice constants. Theoretical and experimental values are included for comparison.

Method	LDA Calculation	a(Å)	c(Å)	c/a	u	B(Mbar)	B'	E_c (eV)	E_g^Γ (eV)
FP-LAPW	Present	3.4975	5.6765	1.623	0.376	1.4919	4.40	8.8524	
AE	Ref. [36]	3.53	5.54	1.57	0.388	1.46	3.4		
	Ref. [28]	3.528	5.684	1.611	0.380	1.41			
PP-GB	Ref. [27]	3.53	5.72	1.620	0.378				-0.4
PP-PW	Ref. [35]	3.544	5.762	1.626	0.377	1.40	6.03	8.694	-0.27
	Ref. [45]	3.524	5.733	1.627	0.377	1.49	4.12	8.799	
	Ref. [40]	3.525		1.613	0.379	1.44	4.6		
HF	Ref. [44]	3.5428	5.7287	1.6170	0.3784				
	GGA Calculation								
FP-LAPW	Present	3.5876	5.8228	1.623	0.377	1.1864	6.03	7.1036	
PP-PW	Ref. [35]	3.614	5.884	1.628	0.377	1.161	7.33	6.872	-0.37
Expt.	Refs. [6][36][44]	3.533	5.693	1.611	0.375	1.25	12.7	7.970	1.9

Table 6: Structural properties and band gap at the Γ point of bulk wurtzite InN, calculated at the theoretical lattice constants. Theoretical and experimental values are included for comparison.

In Figures 6 and 7, the band structure of GaN in the zb and the wz structures is depicted

at the equilibrium lattice constants for the LDA and the GGA, respectively. As in the case of AlN, the band structures appear quite similar. The GGA band gap is 0.411 eV (19.66%) and 0.405 eV (21.07%) smaller than the LDA values for wurtzite and zinc blende structures, respectively. This, as mentioned previously, can be basically attributed to the large GGA lattice constant.

3.3. Indium nitride

Like AlN and GaN, the equilibrium crystal structure of InN is wurtzite but it crystallizes also in the zb structure [6]. We calculate the physical properties of InN in the zb structure as a function of $R_{MT}K_{max}$ and special **k**-points. A convergence of InN properties is quicker than that of GaN, which occurs at and beyond 8.0 for the product of $R_{MT}K_{max}$ and 43 for the special **k**-points in the irreducible part of the Brillouin zone.

In Tables 5 and 6 values of the various bulk properties, listed for the wz and zb structures, are obtained using an $R_{MT}K_{max}$ =9.0 with 114 and 73 special **k**-points, respectively. Our lattice constants obtained by the GGA calculations are 2.58% and 2.06% larger than LDA results, for the wz and the zb structures respectively. Similarly, the bulk modulus is smaller by 20.48% for wz-InN and 16.97% for zb-InN. Compared with experiment, the LDA lattice constant value for the wz structure is 1.00% smaller and the GGA one is 1.55% larger, whereas for the zb structure it is 0.94% smaller for the LDA and 1.11% larger for the GGA. The cohesive energies, similarly to what we found for AlN and GaN, are much smaller when we use the GGA rather than the LDA, by 1.749 eV (19.76%) and 1.847 eV (21.47%), for the wurtzite and the zb structures, respectively. When we compare the calculated cohesive energies to experiment, the GGA values are slightly better than the LDA ones, which is analogous to the differences between LDA and GGA results of AlN and GaN cohesive energies.
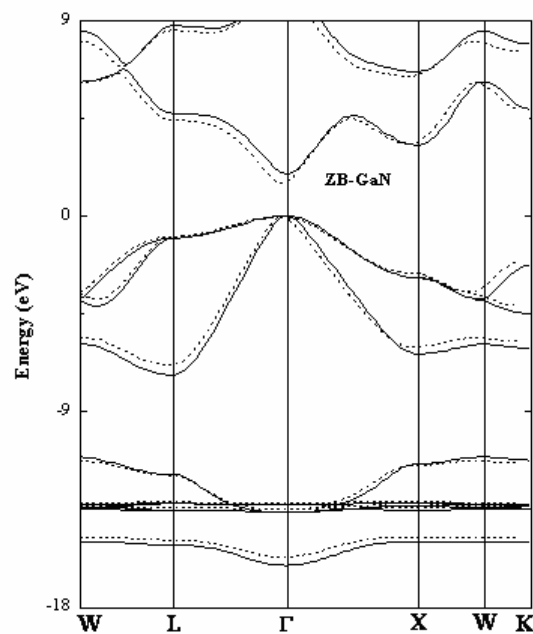

Fig. 6: Band structure at the theoretical lattice constants for zinc-blende GaN as obtained using the LDA (solid curve) and the GGA (dashed curve).
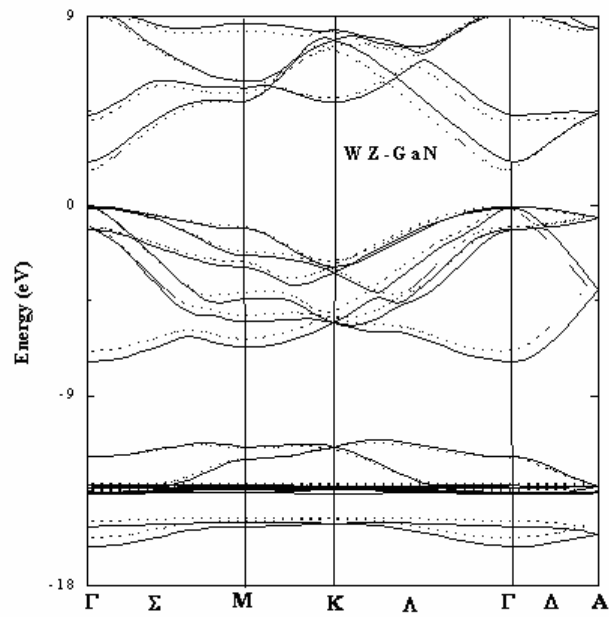
Fig. 7: Band structure at the theoretical lattice constants for wurtzite GaN as obtained using the LDA (solid curve) and the GGA (dashed curve).
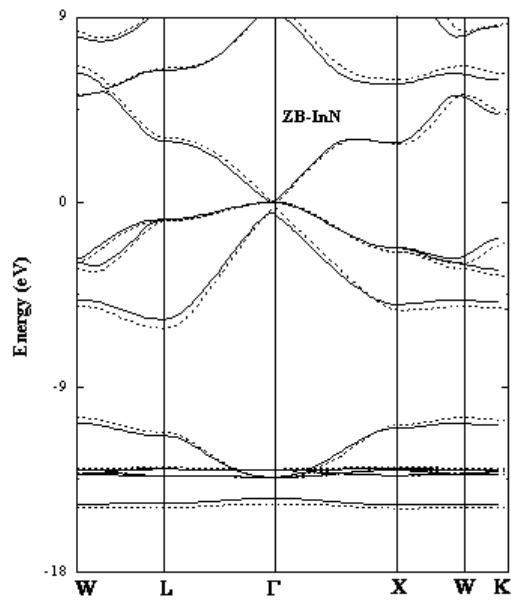

Fig. 8: Band structure at the theoretical lattice constants for zinc-blende InN as obtained using the LDA (solid curve) and the GGA (dashed curve).
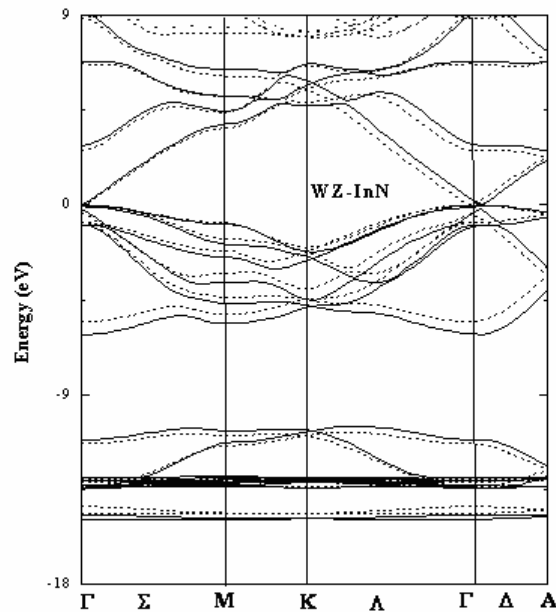
Fig. 9: Band structure at the theoretical lattice constants for wurtzite InN as obtained using the LDA (solid curve) and the GGA (dashed curve).

In Figures. 8 and 9 the band structure of InN in the zb and the wz structures is depicted at the equilibrium lattice constants for the LDA and the GGA, respectively. As in the case of AlN and GaN, the band structures appear quite similar, with no band gap at Γ for LDA and GGA in the zb and wz structures.

By comparing our results with experiment, we find a tendency for the LDA to over bind raise on going from AlN to GaN to InN, while the trend for the GGA was towards decreased under binding on going from GaN to InN to AlN in the zb structure. For the wz structure the degree to which the LDA over binds is larger in GaN than for AlN with InN between, but the tendency of the GGA to under bind increased on going from AlN to GaN to InN. We note some differences between our result and that of Stampfl et al [35] where the degree of under binding in the GGA results for InN under binding is larger than for GaN. The explanation for this is unclear.

The GW quasiparticle [49] and exact-exchange (EXX) Kohn–Sham density functional theory [50] calculations, yields gap energies in reasonable agreement with experiment. The band gaps of these materials are underestimated in the LDA, when compared to the experimental data or GW and EXX calculations (Table). They are 23–45% smaller than the experimental values and this is an intrinsic feature of the DFT-LDA. For InN, where the application of the GW approach is problematic, due the negative LDA bandgap. Theses results are in disagreement with experiment and can be overcome by EXX calculation [50]). However, there is a reported, surprising agreement between LDA and GW results for the valence bandwidths. And it is widely accepted that the LDA electronic band structures are qualitatively in good agreement with the experiments in what concerns the ordering of the energy levels and the shape of the bands. In many cases it is even possible to superimpose LDA electronic bands to the GW or the experimental ones simply with an upwards shift of the theoretical conduction bands [49].

76

3.4. Energy difference between structures

In Table 7 the energy difference between the wz and the zb structures are described and compared to other first-principals calculations. We see a trend of decreasing energy difference on going from AlN to GaN and InN between this trends being the same for all other calculations. However, there are great differences in the magnitude of the energy differences. These are due to the technical details and approximations used in the various calculation methods.

Method	Calculation	AlN	GaN	InN
FP-LAPW	Present (LDA)	40	16	21
	Present (GGA)	43	17	23
AE	Ref. [42]		86.6	
PP-PW	Ref. [35][a] LDA	43.7	8.4	21.4
	Ref. [35][a]	41.6	11.6	17.3
	Ref. [38][a]	42	11	20
	Ref. [48][b]	36.8	19.8	22.9
	Ref. [40][a]	49	10	20
HF	Ref. [44][c]	97.9	35.4	62.6
	Ref. [44][d]	81.6	27.2	40.8

Table 7: The difference in energy *(in meV)* with respect to the zero-pressure wurtzite configuration. Other theoretical values are given for comparison. [a] *d* included as valance states. [b] *d* considered as core states. [c] Electron correlation energy contributions included. [d] Electron correlation energy contributions omitted.

4. Conclusions

We have presented detailed calculations of the bulk properties of the III-V nitrides AlN, GaN and InN in the zinc-blende and wurtzite structures, using the full-potential linearized augmented plane wave (FP-LAPW) approach within the density functional theory (DFT) in the local density approximation (LDA), and the generalized gradient approximation (GGA) for the exchange correlations functional. In addition, we have reported tests of convergence of physical properties as a function of the product $R_{MT}K_{max}$ (where R_{MT} is the average radius of the muffin-tin spheres and K_{max} is the maximum value of the wave vector K=k+G), and the number of special k-points in the irreducible part of the Brillouin zone. We find that using the GGA the lattice constants are 2.58-1.26% larger, bulk modulus 20.48-9.30% smaller and cohesive energy 21.47-12.74% smaller, as compared to the LDA results. The AlN physical properties obtained by the use of the GGA are in good agreement with experimental results, while this is not the case with those of GaN and InN where the LDA results are closer to experiment than those of the GGA. However, the LDA/GGA deviations are very similar for AlN, GaN, and InN in the two structures wurtzite and zinc blende. The GGA presents a tendency for underbinding in these materials, which increases on going from AlN to InN to GaN in the zinc-blende structure and whose principal cause is confusing. For AlN, GaN and InN, the wurtzite structure is the ground-state arrangement, in agreement with experiment. The energy difference between the wurtzite and the zinc blende is found to be largest for AlN

and smallest for GaN. The band structures calculated at the appropriate theoretical lattice constants present some differences between the LDA and the GGA, with smaller band gap for the GGA, which is due fundamentally to the deformation-potential. However, for an III-V nitride material the GGA does not present any improvement as far as the band gap problem is concerned.

III-V nitrides like GaN, InN and AlN and their alloys are becoming increasingly important for the development of optical and high temperature electronic devices due to their wide band gap and high saturation velocity.

References

[1] S. Strite and H. Morkoçe, J. Vac. Sci. Techno. B **10** (1992)1237

[2] C. G. Van De Walle (Ed.), *Wide-band-gap semiconductor*, proceeding of the seventh Trieste semiconductor symposium, North-Holland, Amsterdam (1993); Also published as Physica B **185** (1993).1

[3] H. Morkoçe, S. Strite, G. B. Gao, M. E. Lin, B. Sverdlov, and M. Burns, J. Appl. Phys. **76** (1994) 1363

[4] F. A. Ponce and D. P. Bour, Nature (London) **386** (1997) 351

[5] S. Nakamura, Solid State Commun. **102** (1997) 237

[6] J. H. Edgard (Ed.), *Properties of Group-III Nitrides*, EMIS Data reviews Series, IEE, London (1994)

[7] J. P. Perdew, M. Levy, Phys. Rev. Lett. **51** (1983)1884

[8] L. J. Sham, M. Schlüter, Phys. Rev. Lett. **51**1888 (1983)

[9] J. P. Perdew, A. Chevay, S. H. Vosko, M. R. Pederson, D. J. Singh, C. Fiolhais, Phys. Rev. B **46** (1992) 6671

[10] B. G. Johnson, P. M. W. Gill, J. A. Pople, J. Chem. Phys. **98** (1993) 5612

[11] A. D. Becke, in *The Chalange of d and f Electron*, ACS Symposium Series No. 394, edited by D. R. Salahub and M. C. Zerne, American Chemical Society, Washington DC, page 165 (1989)

[12] A. Garcia, C. Elsaesser, J. Zhu, S. Louie, M. L. Cohen, Phys. Rev. B **46** (1992) 9829

[13] Y. M. Juan, E. Kaxiras, R. G. Gordon, Phys. Rev. B **51** (1995) 9521

[14] A. Dal Corso, A. Pasquarello, A. Baldereschi, R. Car, Phys. Rev. B **53** (1996)1180

[15] M. Körling, J. Häglund, Phys. Rev. B **45**(1992)13 293

[16] P. H. T. Philipsen, G. te Velde, E. J. Baerands, Chem. Phys. Lett. **226** (1994)583

[17] P. Hu, D. A. King, S. Crampin, M. H. Lee, M. C. Payne, Chem. Phys. Lett. **230** (1994)501

[18] D. Porezag, M. R. Pederson, J. Chem. Phys. **102** (1995) 9345

[19] J. Baker, Muir, J. Andzelm, J. Chem. Phys. **102** (1995)2063

[20] P. Dufek, P. Blaha, V. Sliwko, K. Schwarz, Phys. Rev. B **49** (1994)10170

[21] P. Dufek, P. Blaha, K. Schwarz, Phys. Rev. B **50** (1994)7279

[22] T. C. Leung, C. T. Chan, B. N. Harmon, Phys. Rev. B **44** (1991)2923

[23] A. Rubio, J. L. Corkill, M. L. Cohen, E. L. Shirley, S. G. Louie, Phys. Rev. B **48** (1993)11810

[24] M. Palummo, L. Reining, R. W. Godby, C. M. Bertoni, N. Boernsen, Europhys. Lett. **26** (1994) 607

[25] V. Fiorentini, A. Satta, D. Vanderbilt, S. Massidda, F. Meloni, in *the physics of Semiconductors,* edited by D. J. Lock-Wood, Word scientific, Singapore, pp. 137 (1995)

[26] S. J. Jenkins, G. P. Srivastava, J. C. Inkson, Phys. Rev. B **48** (1993) 4388

[27] D. Vogle, P. Krueger, J. Pollmann, Phys. Rev. B **55** (1997)12836

[28] M. Van Schilfgaarde, A. Sher, A. B. Chen, J. Cryst. Growth. **178** (1997) 8

[29] P. Blaha, K. Schwarz, G. K. H. Madsen, D. Kvasnicka, J. Luitz, WIEN2k, *An Augmented Plane Wave + Local Orbital Program for Calculating Crystal Properties,* Karlheinz Schwartz, Techn. Universität Wien, Austria (2001)

[30] J. P. Perdew, S. Burke, M. Ernzerhof, Phys. Rev. Lett. **77** (1996)3865

[31] D. M. Ceperley, G. L. Alder, Phys. Rev. Lett. **45** (1980)566

[32] J. P. Perdew, A. Zunger, Phys. Rev. B **23** (1981)5048

[33] D. D. Koelling, B. N. Harmon, J. Phys. C. Sol. St. Phys. **10** (1977)3107

[34] F. D. Murnaghan, Proc. Natl. Acad. Sci. USA, **30** (1944)244

[35] C. Stampfl, C. G. Van de Walle, Phys. Rev. B **59** (1999)5521

[36] K. Kim, W. R. Lambrecht, B. Segall, Phys. Rev. B **53** (1996)16 310

[37] M. B. Kanoun, A. E. Merad, G. Merad, J. Cebert, H. Aourag, Solid-State Electronics. **48** (2004)1601

[38] A. Satta, V. Fiorentini, A. Bosin, F. Meloni, in *Gallium Nitride and Related Materials*, edited by R. D. Dupuis, J. A. Edmond, F. A. Ponce, and S. Nakamura, MRS Symposia Proceedings No. 395, Materials Research Society, Pittsburgh, pp. 515 (1996)

[39] K. Karch, F.Bechstedt, P. Pavone, D. Strauch, physica B **219** (1996) 445

[40] J. Serrano, A. Rubio, E. Hernandez, A. Muñoz, A. Mujica, Phys. Rev. B **62** (2000)16 612

[41] V. Fiorentini, M. Methfessel, M. Scheffler, Phys. Rev. B **47** (1993) 13 353

[42] N. E. Christensen, I. Gorezyca, Phys. Rev. B **47** (1993)4307

[43] E. Ruiz. S. Alvarez, P. Alemany, Phys. Rev. B **49** (1994) 7115

[44] B. Paulus, F. H. Shi, H. Stoll, J. Phys. Condens. Matter **9** (1997) 2745

[45] A. F. Wright, J. S. Nelson, Phys. Rev. B **51** (1995) 7866

[46] R. Pandey, J. E. Jaffe, N. M. Harrison, J. Phys. Chem. Solids **55** (1994) 1357

[47] R. C. Ppwell, N. E. Lee, Y. W. Kim, J. E. Greene, J. Appl. Phys. **73** (1993) 189 R. C. Ppwell, G. A. Tomasch, Y. W. Kim, J. A. Thornt, J. E. Greene, in *Diamond, Silicon Carbide and Related Wide Band Gap Semiconductors*, edited by J. T. Glass, R. Messier, and N. Fuijimora, MRS Symposia Proceedings No. 162 (Materials Research Society, Pittsburgh, pp. 525, 1990)

[48] C. Y. Yeh, Z. W. Lu, S. Froyen, A. Zunger, Phys. Rev. B **46** 10 086 (1992)

[49] A. Rubio, J. L. Corkill, M. L. Cohen, E. L. Shirley, and S. G. Louie, Phys. Rev. B **48** 11810 (1993)

[50] A. Qteish, A.I. Al-Sharif, M. Fuchs, M. Scheffler, S. Boeck, J. Neugebauer. Computer Physics Communications **169** 28, (2005)